World Applied Sciences Journal 15 (6): 890-898, 2011
ISSN 1818-4952

CFD Modeling of Geometrical Parameters Effects on the Hydrodynamics and Mass Transfer in an Airlift Reactor

Mostafa Keshavarz Moraveji and Reza Davarnejad

Department of Mechanical Engineering,
Science and Research Branch, Islamic Azad University, Arak, Iran

Abstract: In this article, a modeling and a numerical simulation based on the Computational Fluids Dynamic (CFD) method was carried out for two phase flow and mass transfer between gas and liquid phases in an airlift reactor. Further, some reactor geometrical parameters effects such as ratio of height (H_r) to inner diameter (D_r) of draft tube and ratio of inner cross sectional area of riser (A_r) to inner cross sectional area of down comer (A_d) on the system hydrodynamics and mass transfer were investigated. The simulated data was verified with the experimental data obtained from the literature. It was concluded that the simulated data was in good agreement with the experimental one. Gas holdup and liquid circulation velocity showed a maximum at $H_r/D_r = 10.2$ as an optimum point (based on model and experiment). Mixing time was increased with increasing the H_r/D_r ratio. Gas holdup decreased with increasing the A_r/A_d ratio when H_r/D_r values were less than the optimum point. Effect of A_r/A_d on volumetric mass transfer coefficient (K_la) was considered. It concluded that reactor geometrical parameters effect on K_la was ignorable in high and low gas velocities.

Key words: Airlift reactor · Modeling · CFD · Hydrodynamics · Mass transfer · Geometrical parameter

INTRODUCTION

Airlift reactors are one of the important classes of the modified bubble columns which are extensively used as multiphase contactors in various process industries [1, 2]. They are widely used for biological applications because of their ability for providing appropriate hydrodynamics and mass transfer conditions needed for micro-organisms rapid growth [3]. Further, due to their ability for providing an excellent mixing and liquid circulation, they are also applied in wastewater treatment and chemicals production [3, 4].

The Airlift reactors are involved internal and external loop reactors. An internal loop reactor consist of concentric tubes or split vessels if a part of gas is entrained into its down-comer while an external loop one has two conduits connected in top and bottom if little or none gas re-circulates into the down-comer [5].

The dispersion and interfacial mass transfer fluxes are the significant parameters which often limit the overall chemical reaction rates in some systems [1]. These parameters are closely related to the system fluid dynamics, inter-phase mass transfer coefficient and flow turbulence. Since a complex hydrodynamics is observed for some units as their design and scale up will be difficult therefore, an accurate prediction method will be necessary to design an airlift reactor, properly.

A good airlift design requires a comprehensive consideration on geometrical and operating parameters in hydrodynamics and mass transfer processes [6]. Several researches have been conducted on the ratio effect of cross sectional area of riser to cross sectional area of down-comer [7, 8]. Further, the effect of gas liquid separator design in top of a reactor for a gas liquid system was studied [9-11]. According to the literature, the most important parameter in an airlift reactor design and its scale up was the system geometry on a flow with various percentages of phases [6].

A Bubbly flow is involved gas bubbles dispersed in the liquid phase. This flow is prepared in contacting equipments such as mixing tanks, bubble columns and airlift reactors [1, 2].

Corresponding Author: Mostafa Keshavarz Moraveji, Department of Mechanical Engineering, Science and Research Branch, Islamic Azad University, Arak, Iran.
Tel: +98-9363098063.

According to the literature, dynamic breakage and bubbles coalescence have not considered, comprehensively. The bubble size distribution is an important parameter because the interfacial area is a key parameter that controls the Oxygen transfer rate [12]. Since the t hree past decades ago, simulations of gas-liquid two-phase flows in air-lift columns by computational fluid dynamics (CFD) have been started. Several researches have been developed to achieve better control and reliability due to the spectacular progress in digital computing, particularly in CFD, which is reviewed by Sokolichin *et al.* [13]. Most of the researches are chiefly based on two-fluid models, which assume the gas and liquid phases as an interpenetrating media. This is equivalent to Euler-Euler approach. Besides, the Euler-Lagrange approach involves the tracking of individual bubbles in the liquid phase followed by researchers like Sokolichin *et al.* [14] and Delnoij *et al.* [15]. The Euler-Euler approach is more reputed and applicable [16]. In recent years, in order to simulate the gas-liquid and gas-solid flow phase systems, a wide range of CFD studies have been carried out on the air-lift reactors, which are all based on either Euler-Euler or Euler-Lagrange methods [15, 17, 18-24]. The Lagrange Method directly explains the physical interactions between the liquid particles. This method is not applicable in designing large reactors and the systems with a high volume fraction of the dispersed phase.

In the previous work, the effect of the presence of a draft tube on higher rotational movements of gas-liquid in an air-lift reactor using CFD simulation, based on the Euler-Euler method, was studied. Three different layouts for the distance of the draft tube from the wall were examined to determine the optimum situation. According to the results, in a distance of 0.05 m, optimum performance of the reactor was obtained [17].

In the present work, two-dimensional modeling with computational fluid dynamics (CFD) tools is developed based on a two-fluid system, for the simulation of unsteady state flows in an airlift reactor. The objective of this modeling was the effect consideration of the geometrical parameters such as ratio of height (H_r) to inner diameter (D_t) of draft tube, ratio of inner cross sectional area of riser (A_r) to inner cross sectional area of down comer (A_d) on the gas hold up (ε), liquid circulation velocity (V_L), mixing time (t_m) and volumetric mass transfer coefficient (K_la).

Mathematical Modeling: In this work, the Euler-Euler method based on a two-fluid system is employed. The Eulerian-Eulerian two-fluid model is a general and macroscopic model for two phase fluid flow. It treats both phases as interpenetrating media. A velocity zone is associated with each phase. Therefore, a momentum balance and a continuity equation will describe the dynamics of each phase. This method will be applied for average volume fraction of each phase. Therefore, it is not necessary to study every bubble, separately.

The bubbly flow model is a simplified version of two-fluid model. That is related to the following assumptions:

- The motion of the gas bubbles to the liquid is determined by a balance between viscous drag forces and pressure forces.
- The both phases share the same pressure zone.
- A large bubble (heterogeneous flow pattern) usually moves faster than a small bubble, which resulted in breakup and coalescence [25]. As the gas-liquid flow is assumed to be homogeneous (bubbly flow), break-up and coalescence are not considered [26].

Continuity Equation: The continuity equation is derived as following [27]:

$$\frac{\partial(\alpha_k \rho_k)}{\partial t} + \nabla.(\alpha_k \rho_k u_k) = S_k \quad (1)$$

where, α, $\tilde{n}$ and u are gas hold-up, density and velocity in each phase, respectively.

Momentum Equation: The momentum transfer equation is derived as following [27]:

$$\frac{\partial(\alpha_k \rho_k u_k)}{\partial t} + \nabla(\alpha_k \rho_k u_k . u_k) = -\alpha_k \nabla p + \alpha_k \rho_k g + \nabla.\alpha_k \tau_k \pm F_{\text{int}} \quad (2)$$

The right side of the above equation respectively shows pressure difference, gravity force, stress and the ensemble averaged momentum exchange between the intra-phase forces. The pressure is shared between the phases. The drag and lift forces and turbulent stresses model employed in the present study are described in the literature [24].

Constitutive Relations: The transport equation of the volume fraction of gas is given by:

$$\frac{\partial\left(\rho_g \varnothing_g\right)}{\partial_\tau} + \nabla.\left(\rho_g \varnothing_g \mu_g\right) = -m_{gl} \tag{3}$$

For low gas volume fractions ($\phi_g < 0.1$), it is in general valid to replace the continuity equation, Equation (1), by:

$$\nabla.\mu_\xi = 0 \tag{4}$$

The gas phase velocity is obtained as [28]:

$$u_g = u_l + u_{slip} + u_{disp} \tag{5}$$

Where u_{slip} is the relative velocity between the phases and Bubble path dispersion is taken into account by u_{disp} which is proportional to the gas holdup gradient and generally to the turbulent eddy viscosity of the liquid phase [29]. The gas density is obtained from the ideal gas law.

For bubbles rising through a liquid, due to buoyancy, it could be correctly assumed that the pressure forces approximately balance the viscous drag forces on a gas bubble. Hence, the relative velocity between the two phases can be determined from the following relation:

$$\frac{3^C}{4}\frac{D}{d}\rho_L\left|\mu_{Slip}\right|\mu_{Slip} = -\nabla.\mathrm{P} \tag{6}$$

Here d_B denotes the bubble diameter and CD is the viscous drag coefficient for gas bubbles with a diameter larger than 2 mm. An empirical expression for the Jakobsen drag coefficient is [30]:

$$\mathrm{C_D} = \frac{0.622}{\frac{1}{E_o}} + 0.235 \tag{7}$$

Where $E_ö$ is the Eotvos number:

$$E_{\ddot{O}}\frac{g\rho l d_B^2}{\sigma} \tag{8}$$

For bubbles with a diameter smaller than 2 mm, the Hadamard-Rybczynski [31] drag law for spherical gas bubbles in liquid is considered:

$$C_D = \frac{16}{\mathrm{Re}_B} \tag{9}$$

Bubble Reynolds number is given by [32]:

$$\mathrm{Re} = \frac{d_B \rho_l \left|\mu_{mix}\right|}{\mu_l} \tag{10}$$

Turbulence Model: For most of bubbly flow applications, flow zone would be turbulent. In this case, for turbulence effect, k-ε model will be applied. The k-ε model solves two extra transport equations for two additional variables involving the kinetic energy, k, (m^2/s^2) and the dissipation rate of turbulent energy, ε, (m/s^3). The turbulent viscosity can be calculated by following equation:

$$\eta_T = \rho_l C_\mu \frac{k^2}{\varepsilon} \tag{11}$$

where C_i is model constant. The transport equation for the turbulent kinetic energy, k, is as following:

$$\rho_l \frac{\partial k}{\partial t} - \nabla.\left[(\eta + \frac{\eta_k}{\sigma_k})\nabla k\right] + \rho_l u_l.\nabla k = \frac{1}{2}\eta_T(\nabla u_l + (\nabla u_l)^T)^2 - \rho_l \varepsilon + S_k \tag{12}$$

The turbulent energy dissipation rate, ε, will be considered by following equation:

$$\rho_l \frac{\partial \varepsilon}{\partial t} - \nabla.\left[(\eta + \frac{\eta_T}{\sigma_\varepsilon})\nabla \varepsilon\right] + \rho_l u_l.\nabla \varepsilon = \frac{1}{2}C_{\varepsilon 1}\frac{\varepsilon}{k}\eta_T(\nabla u_l + (\nabla u_l)^T)^2 - \rho_l C_{\varepsilon 2}\frac{\varepsilon^2}{k} + \frac{\varepsilon}{k}C_\varepsilon S_k \tag{13}$$

S_k is related to the turbulence status which bubbles motion make it. S_k can be calculated by the following equation:

$$S_k = -C_k \phi_g \nabla P.u_{slip} \tag{14}$$

The turbulent viscosity is taken into account in the momentum equations. Further, a drift velocity should be considered for gas velocity calculation.

$$u_{drift} = -\frac{\eta_T}{\rho_l}\frac{\nabla \phi_g}{\phi_g} \tag{15}$$

The constant values used in the turbulence model are shown in Table 1.

Mass Transfer Modeling: The Oxygen absorption capability in a bioreactor is quantified by the overall volumetric gas-liquid mass transfer coefficient (k_La). Mass transfer between the two phases can be acquired by an expression for the mass transfer rate from the gas to

Table 1: k-ε model constants

Constant	Value
C_i	0.09
$C_{\varepsilon 1}$	1.44
$C_{\varepsilon 2}$	1.92
σ_k	1.00
σs_ε	1.30

Table 2: Reactors geometrical dimensions

	1				2			
Number								
H_r	1.08				1.45			
D_r	0.07	0.10	0.13	0.15	0.07	0.10	0.13	0.15
A_r/A_d	0.16	0.39	0.69	1.38	0.16	0.39	0.69	1.38

liquid. The rate of inter phase mass transfer is proportional to the interfacial area exposed per unit volume and the difference between concentration of dissolved gas at the interface and in the bulk liquid. The higher the interfacial area, the more gas transfers from gaseous phase to liquid phase [25]. The interfacial forces are arisen from momentum transfer across the interface [33]. In order to determine the interfacial area, bubble number density which is number of bubbles per volume should be measured. For this purpose, it was assumed that gas bubbles can expand or shrink (but not completely vanish, merge or split). The conservation of the bubble number density, n, ($1/m^3$) can be calculated by the following equation:

$$\frac{\partial n}{\partial t} + \nabla \cdot \left(n u_g \right) = 0 \tag{16}$$

The mass transfer rate in order to the two-film theory was obtained for dissolution of gas into liquid. The concentration of the dissolved gas can be calculated by the following equation:

$$m_{gl} = K\left(\frac{P + P_{ref.}}{H} - c\right)Ma \tag{17}$$

where:

$$a = \left(4n\pi\right)^{1/3}\left(3\phi_g\right)^{2/3} \tag{18}$$

where, K, H, c, M and a are mass transfer coefficient (m/s), Henry's constant ($Pa.m^3/mol$), concentration of gas dissolved in liquid (mol/m^3), molecular weight (kg/mol) and interfacial area per volume (m^2/m^3), respectively.

The transport equation for dissolved gas is illustrated as following:

$$\frac{\partial c}{\partial t} + \nabla c u_l = \nabla.(D\nabla c) + \frac{m_{gl}}{M} \tag{19}$$

Where, D is the diffusivity coefficient (m^2/s). When a turbulence model is applied for the flow zone, the diffusivity coefficient will be calculated by the following equation:

$$D = \frac{\eta_T}{\rho_1} \tag{20}$$

Mass transfer phenomenon in gas liquid contactors is often expressed by the volumetric mass transfer coefficient ($K_l a$). There are a lot of phenomena contributed to the film mass transfer coefficient (K_l), contact specific area (a) between phases and their combined effects. It is clear these parameters prediction is not easy. For a fundamental consideration on mass transfer phenomenon, separation of K_l and a in the volumetric mass transfer coefficient as first step should be necessary. There are some theories proposed to predict gas liquid mass transfer coefficient. Most of them assume that mass transfer is controlled by the rate of surface renewal as described by Higbie's penetration theory. According to this theory, the liquid phase mass transfer coefficient for a bubble with a mobile surface will be calculated by the following equation:

$$K_l = \frac{2}{\sqrt{\pi}}\sqrt{\frac{Du_{slip}}{d}} \tag{21}$$

Where K_l is liquid side mass transfer coefficient and D is diffusivity coefficient of gas in liquid.

The film mass transfer coefficient K_l is a function of bubble rigidity. If bubble has a mobile interface, $K_{lmobile}$ can be obtained by Higbie's equation which is related to the contact time of liquid bulk around the bubble.

The other model was developed by Kawase [34]. This model is based on average surface renewal rate obtained from contacting bubbles to eddies according to variable contact times. This approach calculates the contact time at various energy dissipation rates and also takes into account interfacial mobility effect which plays a significant role in industrial systems. According to this model, mass transfer coefficient can be obtained by the following equation [34]:

$$K_l = \frac{2}{\sqrt{\pi}}\sqrt{D}\left(\frac{\varepsilon}{\upsilon}\right)^{0.25} \tag{22}$$

The specific interfacial area, a, can be estimated based on the predicted local gas hold up value by the following equation:

$$a = \frac{6a_g}{d_b} \tag{23}$$

where, a_g and d_b are gas hold up and bubble diameter, respectively. In this article Kawase's model [34] was applied to predict mass transfer coefficient.

Numerical Methodology: The governing equations and constitutive relations have been discertized based on finite element method. Discrtized equations have been solved with software package Comsol multiphysics [24]. This software runs the ?nite element analysis alongside with adaptive meshing and error control using a variety of iterative numerical solvers [17,24]. This software generates a mesh that is tetrahedral in shape and isotropic in size. The direct solver UMFPACK is employed because it is preferable for 1D and 2D models. It employs the COLAMD and AMD approximate minimum degree preordering algorithms to permute the columns so that the fill-in is minimized. Boundary conditions for principal equations are assumed to be without slip on the walls. The outlet stream pressure is used as the boundary conditions. At the outlet of the column, the atmospheric pressure was specified as boundary condition. The liquid phase is the continuous phase and the gas phase is presumed dispersant.

The experimental results of Lu *et al.* [35] were used for validation of the model. Three plexiglass reactors have been used in the experiments. Outside diameters (D_r) of 0.07, 0.1, 0.13 and 0.15 m and lengths (H_r) of 1.08 and 1.45 m were used for the round draft tube according to the purposes of different experiments. A single nozzle was located at the base of the riser. In the riser section, air was sparged at superficial gas velocity of 0.02 - 0.1 m s^{-1} based on the entire column cross section.

RESULTS AND DISCUSSION

Effect of H_r/D_r on Hold-Up, Liquid Velocity and Mixing Time: As shown in Fig. 1, the simulation predicts an optimum value for H_r/D_r around 10.2. This output is supported by Weiland [36]. According to this previous research, optimum value for the same parameter when the system had a maximum holdup was at 10.2. The gas holdup values increased with increasing the gas phase velocity (u_g). As shown in the Fig. 2, the same trend was observed for liquid phase velocity (u_l). H_r/D_r increment more than optimum value increased resistant force against liquid flow and therefore, liquid velocity was decreased.

Mixing process will take place according to the turbulence phenomenon and axial dispersion in a reactor. As shown in Fig. 3, H_r/D_r increment (or D_r reduction) will decrease axial dispersion and consequently will decrease mixing time.

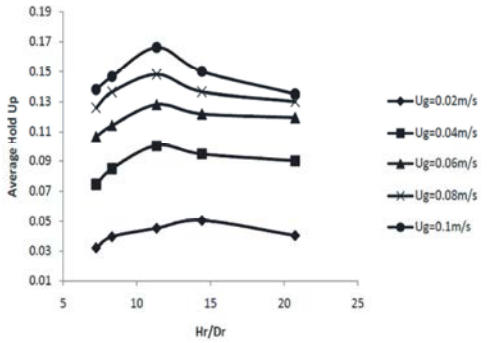

Fig. 1: Effect of Hr/Dr ratio on the average gas holdup versus inlet air velocity

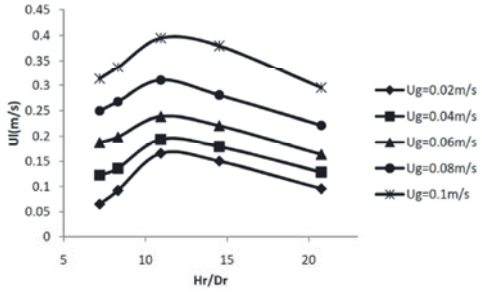

Fig. 2: Effect of H_r/D_r ratio on the liquid circulation velocity versus inlet air velocity

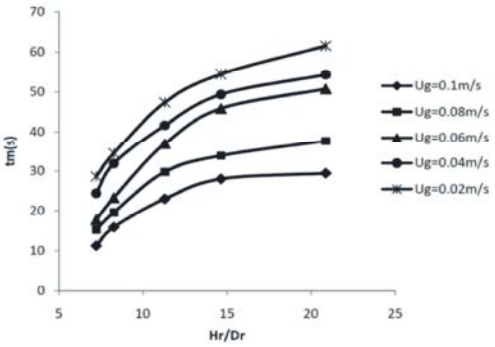

Fig. 3: Effect of H_r/D_r ratio on the mixing time versus inlet air velocity

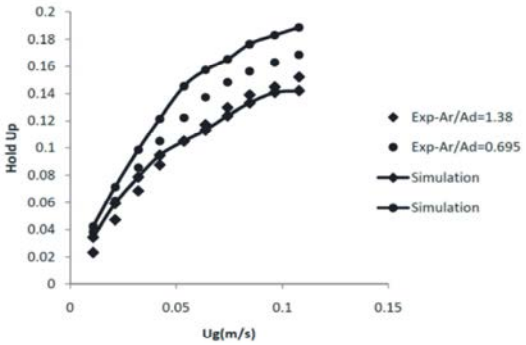

Fig. 4: Effect of A_r/A_d ratio on the gas holdup versus inlet air velocity

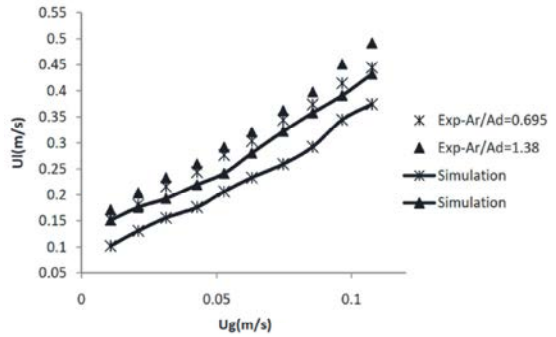

Fig. 5: Effect of A_r/A_d ratio on the liquid circulation velocity versus inlet air velocity

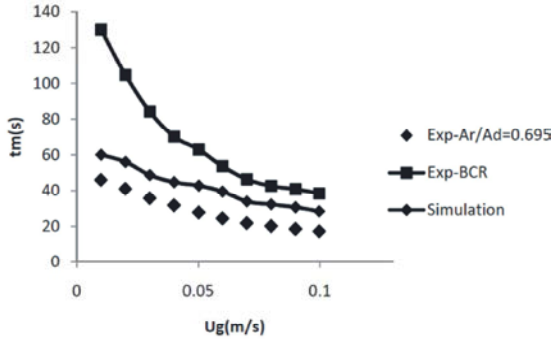

Fig. 7: Comparison of the mixing time versus inlet air velocity in a airlift reactor and bubble column reactor (BCR).

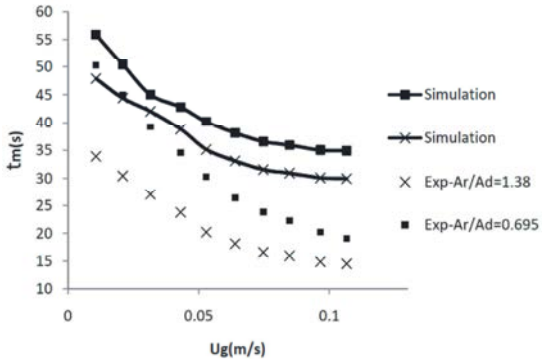

Fig. 6: Effect of A_r/A_d ratio on the mixing time versus inlet air velocity

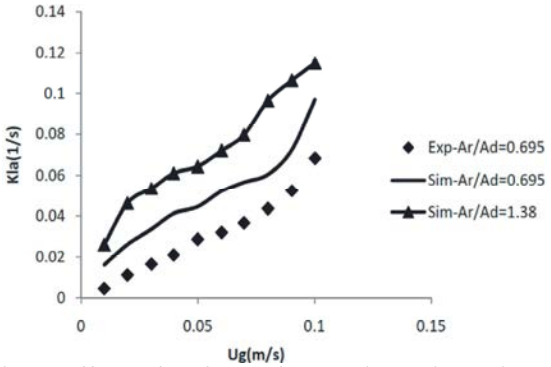

Fig. 8: Effect of A_r/A_d ratio on the volumetric mass transfer coefficient (K_la) versus inlet air velocity

Effect of A_r/A_d: In this section, as example simulation was performed and discussed for H_r/D_r = 8.3 and 7.2 and A_r/A_D = 0.695 and 1.38. Figure 4 shows that gas holdup increases when superficial gas velocity increases. Furthermore, gas holdup values are less for higher values of A_r/A_D. H_r/D_r values which are less than the optimum point cause it. After the optimum point, gas holdup values increase with increasing A_r/A_D values.

Figure 5 shows that as expected, liquid circulation velocity increases with increasing gas velocity. Liquid velocity is more in higher A_r/A_D values. This phenomenon reason is due to having more spaces in riser and holdup increment in it toward total holdup in reactor and consequently driving force increment. As observed, the results obtained from simulation are a bit less than the experimental results. Its reason may be due to missing a proper consideration on bubbles size distribution in this work.

Figure 6 shows that mixing time decrease with increasing u_g and A_r/A_D values. Eddies mixing increase with increasing u_g. According to A_r/A_D, liquid circulation velocity increases with increasing this parameter and consequently the mixing time decreases. These results are supported by Kawase and Moo-young [34]. They expressed that mixing time is increased with A_d increment. As observed in Fig. 6, the simulated data are not matched to the experimental one very well. As already discussed its reason may be due to missing a proper consideration on bubbles size distribution however it is clear that mixing time increases with decreasing liquid velocity.

Figure 7 shows mixing time versus superficial gas velocity. The data obtained from the simulation are compared with the experimental data for an airlift reactor and a bubble column reactor. In a constant gas velocity, mixing time in a bubble column is around two times of mixing time in an airlift reactor.

Figure 8 shows volumetric mass transfer coefficient (K_la) versus gas velocity. The reactor geometrical parameters effect on K_la is ignorable in high and low gas velocities as reported and supported by Lu *et al.* [35]. As observed, in high and low gas velocities K_la values are very close to each other for various A_r/A_D values. Furthermore, K_la increases with A_r/A_D increment. Its reason probably is due to more space in riser and gas hold up increment in it.

CONCLUSIONS

CFD simulation was developed in order to assess the effect of several important geometrical parameters such as H_r/D_r and A_r/A_D on the hydrodynamics and mass transfer characteristics in a airlift reactor. The main hydrodynamic parameters are gas holdup, liquid circulation velocity and mixing time and volumetric mass transfer coefficient is as mass transfer character. The CFD simulation results were finally validated with available experimental data from open literatures.

The gas holdup increased with increasing the A_r/A_D ratio when H_r/D_r was less than the optimum point however it showed an inverse trend for the values which were higher than the optimum point. The liquid velocity increased and consequently mixing time decreased with A_r/A_D increment before the optimum point.

Gas-liquid mass transfer rate depended on the interfacial area per volume unit, as well as the deviation from equilibrium concentration of dissolved gas in liquid. Furthermore, the superficial gas velocity enhancement increased the volumetric mass transfer coefficient.

Nomenclature

Symbols	Description	Unit
A	Contact interfacial area	m^2
Cd	Drag coefficient	--
Cμ	Constant	--
C□1	Constant	--
C□2	Constant	--
C	Dissolved gas concentration	mol/m^3
D	Diffusivity coefficient	m^2/s
db	Bubble diameter	m
G	gravity magnitude	m/s^2
H	Henry's constant	Pa.m3/mol
k	Turbulent kinetic energy	m^2/s^2
K	Mass transfer coefficient	m/s
M	Molecular weight	kg/mol
mgl	Mass transfer rate for gas to liquid	$kg/m^3.s$
n	Number density	1/m3
P	Pressure	Pa
Pref.	Reference pressure	105 Pa
R	Ideal gas constant	8.31 J/mol.K
Sk	The term related to the turbulence status which bubbles motion make it	---
T	Temperature	K
ug	Gas velocity	m/s
ul	Liquid velocity	m/s
uslip	Relative velocity between gas and liquid	m/s
udrift	An additional contribution term when a turbulence model is applied	m/s
Greek letters		
□	Dissipation rate of turbulent energy	m/s^3
η	Mixture viscosity	Pa.s
ηl	Liquid dynamic viscosity	--
ηT	Turbulent viscosity	Pa.s
ρg	Gas density	kg/m^3
ρl	Liquid density	kg/m^3
φg	Gas volume fraction	--
φl	Liquid volume fraction	--
σ	Surface tension coefficient	N/m
σk	Constant	--
σ□	Constant	--
Subscript		
g	Gas	--
l	Liquid	--

REFERENCES

1. Appasani, P., 2007. CFD simulation of the hydrodynamic and inter-phase mass transfer in airlift reactors, DOCTOR OF PHILOSOPHY thesis, Dalhousie University,
2. Pallapothu, S., 2006. Oxygen transfer in airlift reactors equipped with high performance spargers, M.Sc. thesis, Dalhousie University,
3. Couvert, A., D. Bastoul, M. Roustan, A. Line and P. Chatellier, 2001. Prediction of liquid velocity and gas hold-up in rectangular air-lift reactors of different scales. Chem. Eng. Proc., 40: 113-119.
4. Luo, H. and M.H. Al-Dahhan, 2008. Local characteristics of hydrodynamics in draft tube airlift bioreactor, Chem. Eng. Sci., 63: 3057-3068.
5. Fadavi, A. and Y. Chisti, 2007. Gas holdup and mixing characteristics of a novel forced circulation loop reactor, Chem. Eng. J., 131: 105-111.
6. Kilonzo, P.M., A. Margaritis, M.A. Bergougnou, J. Yu and Q. Ye, 2007. Effects of geometrical design on hydrodynamic and mass transfer characteristics of a rectangular-column airlift bioreactor, Biochem. Eng. J., 34: 279-288.
7. Chisti, Y., B. Hallard and M. Moo-Young, 1988. Liquid circulation in airlift reactors, Chem. Eng. Sci., 43(3): 487-494.
8. Popovic, M.K. and C.W. Robinson, 1989. Mass transfer studies of external-loop airlifts and bubble column, AIChE J., 35: 393-405.
9. Siegel, M. and J.C. Merchuk, 1991. Hydrodynamics in rectangular airlift reactors, scale-up and the influence of gas-liquid separator design, Can. J. Chem. Eng., 69: 465-473.
10. Merchuk, J.C. and R. Younger, 1990. The role of gas-liquid separator of airlift reactors in the mixing process, Chem. Eng. Sci., 45(9): 2973-2975.
11. Yazdian, F., S.A. Shojaosadati, M. Nosrati and M. Pesaran Hajiabbas, 2009. Vasheghani-Farahani E. Investigation of gas properties, design and operational parameters on hydrodynamic characteristics, mass transfer and biomass production from natural gas in an external airlift loop bioreactor, Chem. Eng. Sci., 64: 2455-2465.
12. Lo, C.S. and S.J. Hwang, 2003. Local hydrodynamic properties of gas phase in an internal-loop airlift reactor, Chem. Eng. J., 91: 3-32.
13. Sokolichin, A., G. Eigenberger and A. Lapin, 2004. Simulation of buoyancy driven bubbly flow: established simplifications and open questions, AIChE J., 50: 24-45.
14. Sokolichin, A., G. Eigenberger, A. Lapin and A. Lubbert, 1997. Dynamic numerical simulation of gas-liquid two-phase flows Euler/Euler versus Euler/Lagrange, Chem. Eng. Sci., 52: 611-626.
15. Delnoij, E., F.A. Lammers, J.A.M. Kuipers and W.P.M. Van Swaaij, 1997. Dynamic simulation of dispersed gas liquid two-phase flow using a discrete bubble model, Chem. Eng. Sci., 52: 1429-1458.
16. Bhole, M.R., J.B. Joshi and D. Ramkrishna, 2008. CFD simulation of bubble columns incorporating population balance modeling, Chem. Eng. Sci., 63: 2267-2282.
17. Hekmat, A., A.E. Amooghin and M.K. Moravej, 2010. CFD simulation of gas-liquid flow behavior in an air-lift reactor: determination of the optimum distance of the draft tube, Sim. Mod. Prac. Theory, 18(7): 927-945.
18. Lapin, A. and A. Lubbert, 1994. Numerical simulations of the dynamics of two-phase gas-liquid flows in bubble columns, Chem. Eng. Sci., 49: 3661-3674.
19. Devanathan, N., M.P. Dudukovic, A. Lapin and A. Lubbert, 1995. Chaotic flow in bubble column reactors, Chem. Eng. Sci., 50: 2661-2667.
20. Lain, S., D. Broder and M. Sommerfeld, 1999. Experimental and numerical studies of the hydrodynamics in a bubble column, Chem. Eng. Sci., 54: 4913-4920.
21. Buwa, V.V., D.S. Deo and V.V. Ranade, 2006. Eulerian-Lagrangian simulations of unsteady gas-liquid flows in bubble columns, Int. J. Multiphase Flow, 32: 864-885.
22. Azizi, S., S.H. Hosseini, M.K. Moraveji and G. Ahmadi, 2010. CFD modeling of a spouted bed with a porous draft tube, Particuol., 8: 415-424.
23. Azizi, S., S.H. Hosseini, M.K. Moraveji and G. Ahmadi, 2010. Numerical Simulation of Particle Segregation in Bubbling Gas-Fluidized Beds, Chem. Eng. Technol., 33: 421-432.
24. Moraveji, M.K., B. Sajjadi, M. Jafarkhani and R. Davarnejad, 2011. Experimental investigation and CFD simulation of turbulence effect on hydrodynamic and mass transfer in a packed bed airlift internal loop reactor, Int. Comm. Heat and Mass Trans., 38: 518-524.

25. Kommareddy, A. and G. anderson, 2004. Analysis of Currents and Mixing in a modified Bubble Column Reactor, CSAE/ASAE Annual Intersectional Meeting, USA,
26. Zhang, D., J.A.M. Deen and J.A.M. Kuipers, 2005. Numerical Simulation of Dynamic Flow Behaviour in a Bubble Column: Comparison of the Bubble-Induced Turbulence Models in the k-ε Model, Fourth International Conference on CFD in the Oil and Gas, Metallurgical & Process Industries SINTEF / NTNU Trondheim, Norway,
27. Cartland Glover, G.M., S.C. Generalis and N.H. Thomas, 2000. CFD and Bubble Column Reactors: Simulation and Experiment, Chem. Pap., 54: 361-369.
28. Kuzmin, D. and S. Turek, 2000. Efficient numerical techniques for flow simulation in bubble column reactors. in Preprints of the 5th German-Japanese Symposium on Bubble Columns, VDI/GVC, pp : 99-104.
29. Kuzmin, D., 1999. Numerical Simulation of Reactive Bubbly Flows. Dissertation. Jyvaskyla Studies in Computing,
30. Jakobsen, H.A., B.H. Sannaes, S. Grevskott and H.F. Svendsen, 1997. Modelling of vertical bubble-driven flows, Ind. Eng. Chem. Res., 36: 4052-4074.
31. Crowe, C., M. Sommerfeld and Y. Tsuji, 1999. Multiphase Flows with Droplets and Particles. CRC Press,
32. Blazej, M., G.M. Cartland Glover, S.C. Generalis and J. Markos, 2004. Gas-liquid simulation of an airlift bubble column reactor, Chem. Eng. Process. 43: 137-144.
33. Dhotre, M.T. and J.B. Joshi, 2007. Design of a gas distributor: Three-dimensional CFD simulation of a coupled system consisting of a gas chamber and a bubble column, Chem. Eng. J., 125: 149-163.
34. Kawase, Y. and M. Moo-Young, 1986. Mixing and mass transfer in concentric tube airlift fermenters: Newtonian and non-Newtonian media, J. Chem. Technol., 36: 527-533.
35. Lu, X., J. Ding, Y. Wang and J. Shi, 2000. Comparison of the hydrodynamics and mass transfer characteristics of a modified square airlift reactor with common airlift reactors, Chem. Eng. Sci., 55: 2257-2263.
36. Weiland, P., 1984. Influence of draft tube diameter on operator behavior of air-lift loop reactor, German Chem. Eng., 7: 374-385.